Analysis of the Performance of the I-V Curve Correction Methods in the Presence of Defects

Baojie Li, Anne Migan-Dubois, Claude Delpha, Demba Diallo

ANALYSIS OF THE PERFORMANCE OF I-V CURVE CORRECTION METHODS IN THE PRESENCE OF DEFECTS

Baojie LI[1,2], Anne MIGAN-DUBOIS[1*], Claude DELPHA[2], Demba DIALLO[1],
[1] Université Paris-Saclay, CentraleSupélec, CNRS, GeePs, Sorbonne Université, 3-11 Rue Joliot Curie, Gif Sur Yvette, 91192, France
[2] Université Paris-Saclay, CNRS, CentraleSupélec, L2S, 3 Rue Joliot Curie, Gif Sur Yvette, 91192, France

ABSTRACT: Photovoltaic I-V curve contains rich information about the status of the PV module or array. Therefore, the I-V curve-based PV diagnosis has always been a popular issue, especially with the solutions of the I-V curve measurement at module or array level becoming commercially-available in recent years. Among the I-V curve-based diagnosis applications, the correction of I-V curves measured under various environmental condition to an identical condition is usually a crucial step. However, there is no specific method dedicated to the correction of faulty I-V curves. Therefore, the correction procedures proposed in IEC 60891 standard are commonly adopted, which, however, have only been validated for the correction of curves measured for healthy PV module or array. Consequently, this paper is conceived to evaluate the performance of the IEC 60891 single curve-based methods (procedure 1 and 2) for the correction of faulty I-V curves. Five types of fault conditions of a PV array are addressed. The correction methods are tested using three groups of I-V curves simulated difference irradiance and module temperature. Their impact on the correction performance are specially analyzed. Suggestions for the selection of procedure 1 or 2 under different conditions are given at the end.

Keywords: I-V curve, I-V curve correction, IEC 60891, fault detection and diagnosis, photovoltaic

1 INTRODUCTION

In order to improve health monitoring of photovoltaic (PV) devices, several PV arrays have decided to implement hardware solutions to measure the I-V curve periodically at inverter level [1,2], or for some reference modules that are placed near the array and are equipped with I-V tracer to interpret the condition of the whole array [3]. Therefore, I-V curve-based PV diagnostic has become a popular issue [4]. However, when using the field measured I-V curve for diagnostic, one important step is to correct the curves measured at random irradiance (G) or temperature (Tm) to the standard test condition (STC). This correction, not only allows the comparison chronologically to analyze the degradation rate [3], but also allows the comparison with the healthy I-V curve provided by the manufacturer or obtained with an indoor solar simulator. The comparison results are then used to identify the common electrical faults, like partial shading (PS), open-circuit (OC) and short-circuit (SC) [5].

In the literature, the common correction methods are of the single I-V curve-based type, which means the correction could be conducted even if only one I-V curve is available [6,7]. This type of method is suitable for fast field correction. And among these methods, the procedure 1 and 2 proposed in IEC 60891 standard [8] are the basic and the most common ones. However, these methods are initially designed for the correction of I-V curves measured for the healthy modules. When the module or array is in faulty condition, it is unclear whether these correction methods will induce an error that will distort the fault severity estimation. Thus, the objective of this paper is to evaluate this correction performance under faulty condition when using the IEC correction procedures 1 and 2.

2 METHODOLOGY

Since our aim is to evaluate the correction error caused by the I-V curve correction methods, it is essential to avoid the effects of other uncertainty factors, especially the measurement biases of environmental and electrical parameters. Therefore, our study is based on simulated data to carry on the correction analysis.

2.1 Simulation of I-V curves

A PV array model with 6 monocrystalline silicon (sc-Si) modules (2 parallel strings, each string has 3 modules in series) is developed under Simulink® as shown in Figure 1. The module parameters are listed in Table I.

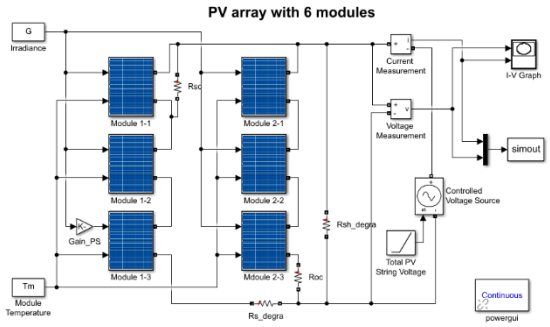

Figure 1: Simulation model of a PV array with 6 modules

Table I: Parameter setting of sc-Si PV module

Variable	Value	Variable	Value
I_{SC}	8.64 A	V_{MPP}	31.80 V
V_{OC}	37.90 V	α_{rel}	0.02 %/°C
I_{MPP}	6.52 A	β_{rel}	-0.36 %/°C

All the modules have same module temperature (Tm) and receive identical irradiance (G). However, under partial shading (PS) condition the shaded module receives an irradiation equal to $G \times GainPS$ ($GainPS$ is a parameter to control the PS level, the value is in [0, 1]).

The model can simulate PV array under healthy and several faulty conditions including one shaded module (PS), 1 short-circuited (SC) module thanks to resistance R_{SC} (connected to 1 module in parallel), 1 open-circuit

(OC) string thanks to the series-connected resistance R_{OC}, array series resistance degradation (resistance *Rs*) and array shunt degradation (resistance Rsh). The parameter settings for the different conditions are shown in Table II.

Table II: Parameter setting to set the different conditions

Condition	GainPS	R_{SC} (Ω)	R_{OC} (Ω)	Rs (Ω)	Rsh (Ω)
Healthy	1	10^6	10^{-6}	10^{-6}	10^6
PS 1 module	**0.2**	10^6	10^{-6}	10^{-6}	10^6
SC 1 module	1	**10^{-6}**	10^{-6}	10^{-6}	10^6
OC 1 string	1	10^6	**10^6**	10^{-6}	10^6
Rs degradation	1	10^6	10^{-6}	**1**	10^6
Rsh degradation	1	10^6	10^{-6}	10^{-6}	**30**

The *G* and *Tm* of the simulated curve to correct are ones of the critical variables in the correction. Therefore, it is essential to evaluate the correction performance using curves with different *G* and *Tm*. To this end, *G* and *Tm* in simulation are varied with different values and build up 3 groups of curve data with the setting presented in Table III. Group 1 (*Tm* constant, *G* varies in the presented range with a fixed step) and group 2 (*G* constant, *Tm* varies) are applied to investigate the independent impact of *G* or *Tm*, respectively. As in the real case, in order to minimize the correction error, the *G* of the curves for correction are always selected at a high range [9]. Therefore, for group 1, the lower bound of *G* is set as 800 W/P2. While for *Tm*, there is no limit with a relatively wide range adopted for group 2.

In fact, *G* and *Tm* of group 1 and 2 are not common in the real case. Thus, group 3 is created with *G* and *Tm* both varying but within the field measurement range as illustrated in Figure 2. In Figure 2, the blue points represent the measured *G* and *Tm* in the summer of the same sc-Si module [10,11] as those used in the simulation. Within the area enclosed by these points, the *G* and *Tm* for group 3 (red points) are accordingly uniformly selected.

Table III: Simulation setting of 3 groups of I-V data

Data group	*G* range (W/P2)	*Tm* range (°C)	Usage
Group 1	[800, 1200]	25	Evaluate the impact of *G*
Group 2	1000	[10, 80]	Evaluate the impact of *Tm*
Group 3 (field-measured *G* and *Tm*)	[800, 1150]	[42, 75]	Evaluate the performance at random *G* and *Tm*

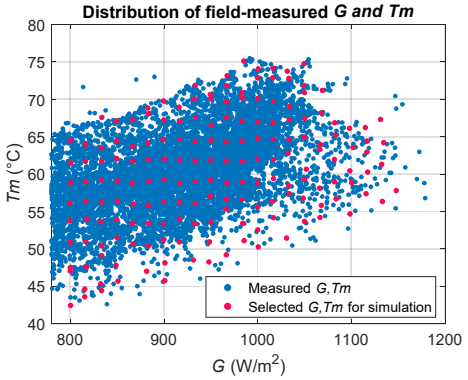

Figure 2: Selected *G* and *Tm* (group 3) based on field measurement

2.2 Correction methods

In this study, the procedures 1 and 2 proposed in IEC 60891are addressed, which are detailed as follows:

- Procedure 1 (P1):

$$I_2 = I_1 + I_{SC1}(G_2/G_1 - 1) + \alpha(T_{m2} - T_{m1}) \quad (1)$$

$$V_2 = V_1 - R_s(I_2 - I_1) - \kappa I_2(T_{m2} - T_{m1}) + \beta(T_{m2} - T_{m1}) \quad (2)$$

where, I_1 and I_2, V_1 and V_2, T_{m1} and T_{m2}, G_1 and G_2 are the current, voltage, *Tm* and *G* before and after correction, respectively; I_{SC1} is the short-circuit current (I_{sc}) before correction; α and β are the PV module absolute temperature coefficient (TC) of I_{sc} and open-circuit voltage (V_{oc}) respectively; $\alpha = \alpha_{rel} \cdot I_{sc}^{STC}$, $\beta = \beta_{rel} \cdot V_{oc}^{STC}$, α_{rel} and β_{rel} are the relative TC of I_{sc} and V_{oc}; R_s is the internal series resistance and κ is the curve correction factor.

- Procedure 2 (P2):

$$I_2 = I_1(1 + \alpha_{rel}(T_{m2} - T_{m1}))G_2/G_1 \quad (3)$$

$$V_2 = V_1 + V_{oc1}\left(\beta_{rel}(T_{m2} - T_{m1}) + a \cdot ln\left(\frac{G_2}{G_1}\right)\right) - R_s(I_2 - I_1) - \kappa \cdot I_2(T_{m2} - T_{m1}) \quad (4)$$

where, V_{oc1} is the V_{oc} of the curve to correct; a is the irradiance correction factor; R_s and κ may not be of the same value used in P1, but determined by tuning.

In real application case, when the PV module or array condition is unknown, the measured I-V curves are generally corrected using the parameters identified in healthy condition [12]. Therefore, in our research, the aforementioned parameters of P1 and P2 are also tuned under healthy condition. These tuned correction methods serve as the pre-diagnostic tools for PV devices.

2.3 Performance evaluation metric

To evaluate the correction performance for the whole I-V curve, the curve error ($E_{I\text{-}V}$) is adopted as the metric. $E_{I\text{-}V}$ is calculated by the normalized root-mean-square error between the corrected curve and simulated-at-STC curve (hereinafter called real curve) as in (5). It should be noted that the real curve only means that the *G* and *Tm* are at STC, but the array condition could be either healthy or faulty.

$$E_{I-V} = \frac{\sqrt{\frac{1}{N}\sum_{i=1}^{N}(I_i^c - I_i^{real})^2}}{I_{sc}^{real}} \quad (5)$$

where, I_i^c and I_i^{real} are the current value interpolated at voltage V_i on the corrected and real curve; V_i is the i^{th} element of a voltage vector linearly interpolated in $[0, V_{max}]$ with N points by a fixed step (V_{max} is a constant for all the conditions, which could be set a little larger than the array V_{oc} at STC in healthy condition to avoid the voltage of improperly-corrected curve exceeding this range, here, V_{max} is set as 120V and N is 100); I_{sc}^{real} refers to the I_{sc} extracted from the real curve.

3 CORRECTION PERFORMANCE

In this section, the I-V curves simulated at the 3 groups of settings for *G* and *Tm* (presented in Table III) are adopted to evaluate the correction performance of P1 and P2.

3.1 Impact of *G* on the correction performance

Taking the group 1 curves (simulated at same *Tm*, different *G*), the corrected curves using P1&P2 and the relationship of the corresponding $E_{I\text{-}V}$ with *G* are presented

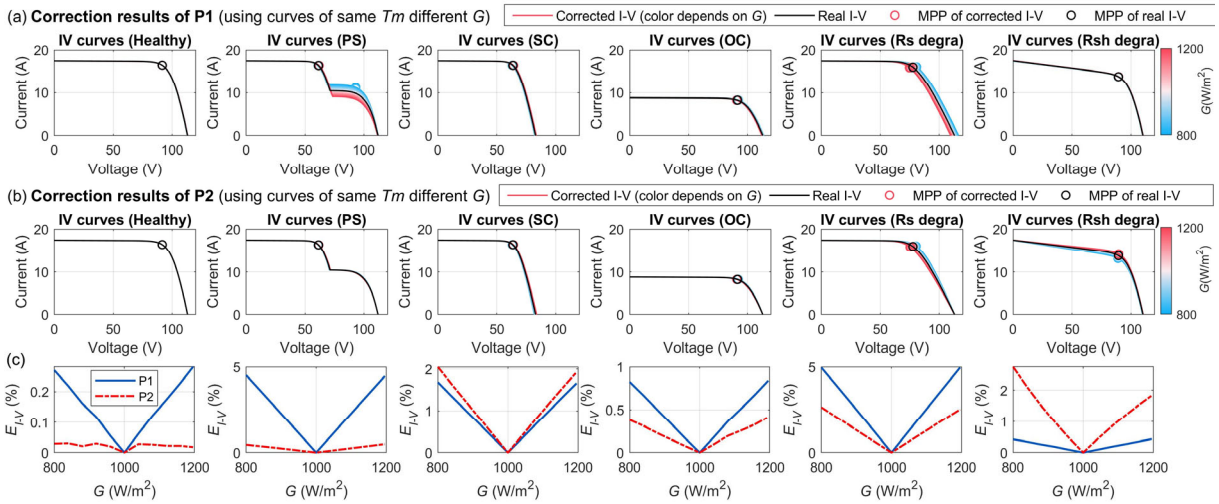

Figure 3 Impact of G on correction performance based on I-V curves of same Tm and different G: (a) corrected I-V curves using P1, (b) corrected I-V curves using P2, (c) comparison of CE using P1 and P2

in Figure 3.

Regarding the corrected curves, with the variation of G, P1 and P2 could both keep the right curve shape after the correction under most conditions, except for PS using P1 and Rs degradation using both methods. Besides, it is observed that, globally, $E_{I\text{-}V}$ increases linearly with G deviating from 1000W/P2 for both methods and therefore exhibits a quasi-symmetric 1000W/P2-centred 'V shape' form. This is logical as all the curves are corrected to 1000W/P2 and $E_{I\text{-}V}$ quantifies the absolute error with the value constantly positive. That is also why, in real application cases, it is favored to select data measured near the G at STC for correction, as the error will be lower.

3.2 Impact of Tm on the correction performance

Based on the group 2 curves (simulated at same G, different Tm), the corrected curves and the $E_{I\text{-}V}$ as a function of Tm is presented in Figure 4.

With respect to the corrected curves, for P1, clear discrepancy between corrected and real curves could be observed for PS, SC and Rsh degradation. In other conditions, the curves appear well-overlapped. However, for P2, the noticeable discrepancy could be recognized for all conditions, even under healthy one. Besides, a clear discrepancy near the open-circuit area is common for nearly all the conditions for P2. These phenomena are supposed to be mainly due to the improper correction of voltage in these two methods.

As for $E_{I\text{-}V}$, it still exhibits a linear relationship with Tm when using P1, while using P2, the shape of $E_{I\text{-}V}$ is relatively irregular. Nevertheless, for both methods, $E_{I\text{-}V}$ comes to 0 when Tm=25°C and increases with Tm getting away from 25°C.

3.3 Correction using data with variable G and Tm

In this subsection, the group 3 curves are adopted. It should be noted that the G and Tm of these curves are no longer independently varying as in group 1 or 2, but are based on field measurements. This means, higher G will generally result in higher Tm. In this way, P1 and P2 could be evaluated by the curves more commonly encountered in the real case. Now, the curves before and after correction are presented in Figure 5.

From Figure 5, it is observed that the corrected curves reflect the joint impact of G and Tm for both methods, which have been analyzed in Section 3.1 and 3.2. In this sense, intuitively, except for the healthy and OC case using

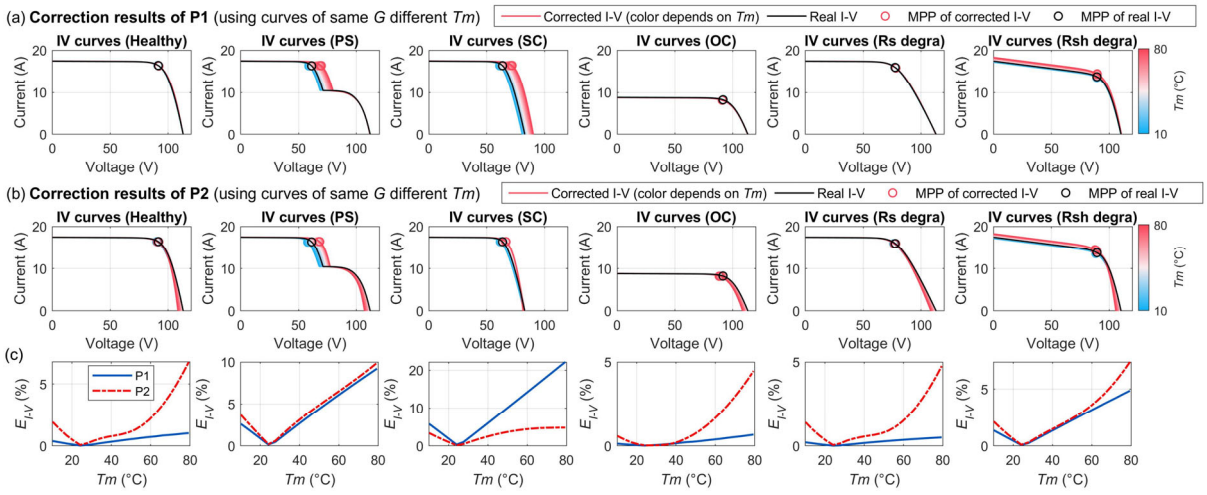

Figure 4: Impact of Tm on correction performance based on I-V curves of same G and different Tm: (a) corrected I-V curves using P1, (b) corrected I-V curves using P2, (c) comparison of $E_{I\text{-}V}$ using P1 and P2

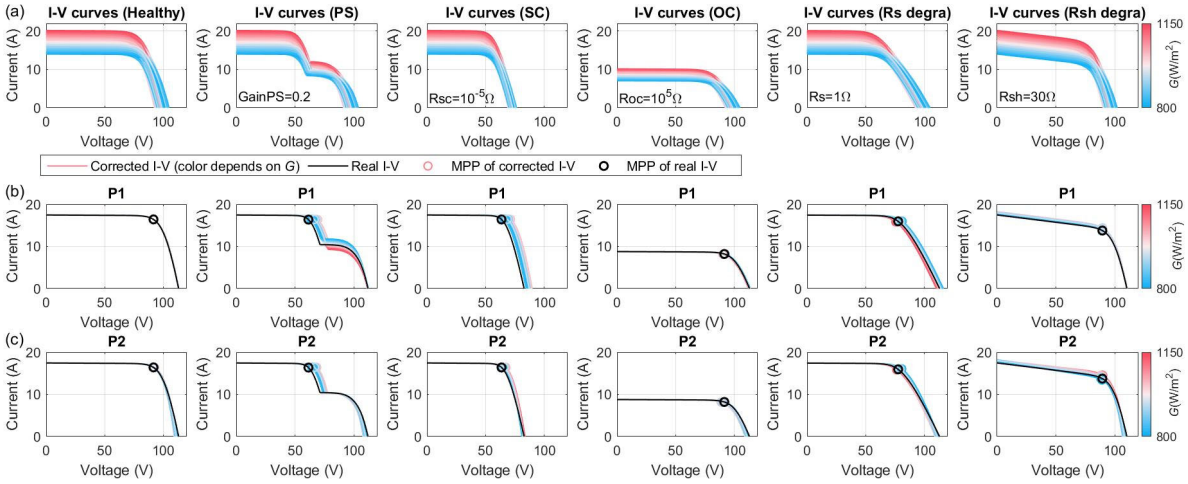

Figure 5: Correction results using group 3 curves, (a): curves simulated for correction (each condition contains curves with field-measured combinations of *G* and *Tm* at constant fault severity), (b): corrected curves using P1, (c): corrected curves using P2 (the displayed color of each curve is determined by the *G* of the curve with the colorbar shown at the right side of the figure)

P1, clear non-overlapping could be observed for all other cases. Using the statistical method, the $E_{I\text{-}V}$ of these curves for P1 and P2 is presented in Figure 6.

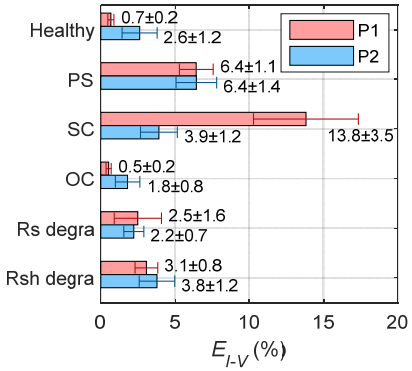

Figure 6: $E_{I\text{-}V}$ using P1 and P2 under all conditions (the bars represent the mean CE of corrected curves, while the horizontal lines represent the standard deviation)

Based on $E_{I\text{-}V}$, which reflects the correction error on the whole curve, P1 and P2 exhibit similar results under most conditions. Large $E_{I\text{-}V}$ (up to 13.8%) is observed for P1 under SC, which corresponds to the observed large deviation of corrected curves near V_{oc} as shown Fig. 5 (b). This significant error is supposed to be due to the poor correction of voltage of P1 when the V_{oc} of the current condition changes, like under OC.

It should be noted that, neither P1 nor P2 could reach the best performance under all the conditions. However, globally, the performance of P2 is relatively more robust.

As for whether the fault features or severity are changed after correction, the features like the reflection point for *PS*, the steep slope for Rsh degradation are all retained on the corrected curves. However, when using P1 the inflection point, the MPP using P1 or P2, are all likely to be shifted when the curve is measured under conditions too different from STC. This inevitably will lead to an error for the fault severity estimation.

4 DISCUSSION

As observed, the studied 2 single curve-based correction methods all fail to fit well all the tested faulty conditions. Nevertheless, when the condition of one PV module or array could be roughly estimated, based on $E_{I\text{-}V}$, there come suggestions for the choice of method, which are listed in Table IV.

Additionally, as can be observed from the correction formula (1-4), closer to STC, better correction performance. However, in real condition, the optimum of

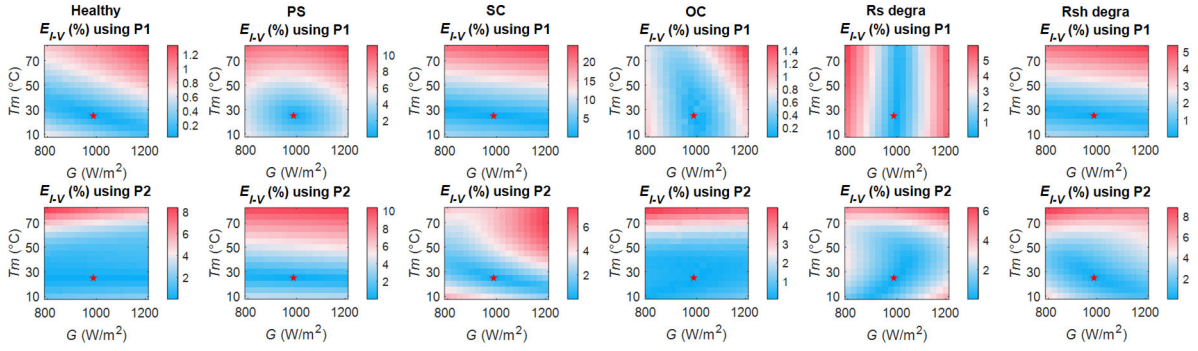

Figure 7: Comparison of sensibility of $E_{I\text{-}V}$ to *G* and *Tm* using P1 and P2 ($E_{I\text{-}V}$ is presented in colormap, STC is presented in red star)

both *G* and *Tm* is troublesome [13]. Nevertheless, for a given method, its performance sensibility to *G* and *Tm* could be compared. In this sense, when simultaneous optimum of *G* and *Tm* is impossible, we could give suggestions to prioritize the optimum of which environmental factor. These suggestions (also presented in Table IV) are made based on the sensibility analysis of $E_{I\text{-}V}$ to *G* and *Tm*, which is presented in Figure 7. When $E_{I\text{-}V}$ varies more quickly to one factor, this means it is more sensitive to this factor. Therefore, this factor should be paid more attention to when the environmental condition or measurement time for the curve to correct is able to be adjusted.

Table IV: Suggestions for single curve-based correction method and prior optimum of the environmental factor under each condition

Case	Suitable method	Prior optimization
Healthy	P1	*Tm*
PS	P2	*Tm*
SC	P2	*Tm*
OC	P1	*G*
Rs degra	P2	*Tm*
Rsh degra	P1	*Tm*

5 CONCLUSION

Through the comparison of the IEC 60891 single I-V curve-based correction methods, it is found that none of them could fit all the tested faulty conditions well. Nonetheless, P2 is relatively more stable and accurate for the correction of curves under the tested faulty conditions. When the fault condition is known or could be roughly estimated, suggestions for the selection of methods is given. Future work will be to quantify the fault severity estimation after correction and evaluate the performance with varying fault severity. Besides, other correction methods will also be tested and analyzed, so as to finally propose an accurate and robust method to correct measured I-V curves of PV module or array under faulty conditions.

ACKNOWLEDGEMENT

The author would like to thank the China Scholarship Council for the funding of the PhD.

REFERENCES

[1] Spataru S, Sera D, Kerekes T, Teodorescu R. Monitoring and Fault Detection in Photovoltaic Systems Based On Inverter Measured String I-V Curves. 31st European PV Solar Energy Conference and Exhibition (Eu-PVSEC), Hamburg, Germany; 14-18 Sept. 2015, p. 1667–74.

[2] Phinikarides A, Kindyni N, Makrides G, Georghiou GE. Review of photovoltaic degradation rate methodologies. Renew Sustain Energy Rev 2014; 40: 143–52.

[3] Bouaichi A, Alami A, Hajjaj C, Messaoudi C, Ghennioui A, Benlarabi A, et al. In-situ evaluation of the early PV module degradation of various technologies under harsh climatic conditions : The case of Morocco. Renew Energy 2019; 143: 1500–18.

[4] Mellit A, Tina GM, Kalogirou SA. Fault detection and diagnosis methods for photovoltaic systems: A review. Renew Sustain Energy Rev 2018; 91: 1–17.

[5] Livera A, Theristis M, Makrides G, Georghiou GE. Recent advances in failure diagnosis techniques based on performance data analysis for grid-connected photovoltaic systems. Renew Energy 2019; 133: 126–43.

[6] Hishikawa Y, Takenouchi T, Higa M, Yamagoe K, Ohshima H, Yoshita M. Translation of Solar Cell Performance for Irradiance and Temperature from a Single I-V Curve Without Advance Information of Translation Parameters. IEEE J Photovoltaics 2019; 9: 1195–201.

[7] Bühler AJ, Perin Gasparin F, Krenzinger A. Post-processing data of measured I–V curves of photovoltaic devices. Renew Energy 2014; 68: 602–10.

[8] IEC 60891. Photovoltaic devices - Procedures for temperature and irradiance corrections to measured I-V characteristics. 2009.

[9] Ding K, Zhang J, Bian X, Xu J. A simplified model for photovoltaic modules based on improved translation equations. Sol Energy 2014; 101: 40–52.

[10] Migan A, Mambrini T, Bourdin V, Badosa J. Deployment of a multi-technology photovoltaic module test bench on the SIRTA meteorological and climate observatory. 31st European PV Solar Energy Conference and Exhibition (Eu-PVSEC), Hamburg, Germany; 14-18 Sept. 2015.

[11] Dubois AM, Badosa J, Calderon-Obaldia F, Atlan O, Bourdin V, Pavlov M, et al. Step-by-step evaluation of photovoltaic module performance related to outdoor parameters: evaluation of the uncertainty. 2017 IEEE 44th Photovoltaic Specialist Conference (PVSC), Washington, DC, USA; 25-30 June 2017, p. 626–31.

[12] Quansah DA, Adaramola MS. Ageing and degradation in solar photovoltaic modules installed in northern Ghana. Sol Energy 2018; 173: 834–47.

[13] Duck BC, Fell CJ, Marion B, Emery K. Comparing standard translation methods for predicting photovoltaic energy production. 2013 IEEE 39th Photovoltaic Specialists Conference (PVSC), Tampa, USA; 16-21 June 2013, p. 0763–8.